

Photometric observations of six Mars-crossing asteroids with the 1-m INASAN telescope at Mt. Koshka

A.S. Kravtsova^{1,2}, S. I. Barabanov² and I.M. Volkov^{1,2}

¹ *Sternberg Astronomical Institute, Lomonosov Moscow State University, Universitetskij Ave. 13, 119992 Moscow, Russia (E-mail:*

kravts@yandex.ru, hwp@yandex.ru)

² *Institute of Astronomy of the Russian Academy of Sciences, 48 Pyatnitskaya street, 119017 Moscow,*

Russia (E-mail: sbarabanov64@yandex.ru)

Received: June 24, 2022; Accepted: October 6, 2022

Abstract. We present observations of six asteroids crossing the orbit of Mars obtained at Mt. Koshka observatory of INASAN in 2014–2016. Our multicolor photometry made it possible to determine the apparent magnitudes of asteroids in *BVRcIc* photometric bands, as well as their taxonomic class according to Tholen’s classification. The periods of rotation were determined for asteroids 9773, 32575, 97679, and 313591. For asteroid 8355 Masuo the rotation period determined earlier was confirmed. Our observations support the long period of rotation for asteroid 122463 (presumably about 19 days).

Key words: asteroids: photometry – asteroids: Tholen classification

1. Introduction

Since 2010, multicolor observations of asteroids have been carried out at the 1-m telescope in Simeiz. The most important asteroids are those approaching the Earth’s orbit (NEA). However, not a lot of NEA have a sufficient brightness to obtain high-quality multicolor photometric observations. So we choose objects from much more numerous Mars-crossing asteroids which are related to the NEA group. These asteroids in some cases can cross the Earth’s orbit or approach the Earth. NEA and Mars-crossing asteroids can move from one group to another due to orbit changing. It is important to investigate the taxonomy and rotation of Mars-crossing asteroids, compare them to NEA and follow the evolution of their orbits.

Mars-crossing asteroids are also interesting because of their connection to Mars. Automatic vehicles are visiting Mars’ orbit and go down to its surface. Small objects associated with Mars, such as meteor showers and fireballs, can seriously interfere with the work of automatic stations exploring its surface and, in the future, inhabited settlements. We must have comprehensive information

about the physical and mineralogical properties of near-Martian asteroids. Some of them can be in future a source of industrial minerals.

2. Observations

Thoroughly calibrated photometric systems make it possible to obtain reliable data on the physical and mineralogical features of the small bodies in Solar System.

Our photometrical multicolor observations were carried out with a Zeiss-1000 cassegrain ($D = 1$ m, $f/12.7$) in the Simeiz observatory of INASAN. An FLI PL-09000 (3056x3056) CCD array was equipped with a *BVRcIc* filter set which realized the Johnson-Cousins photometric system. 5x5 binning provided a 0.97" pixel size. Seeing was usually 3-4". More information about the observatory and telescope one may find in [Nikolenko et al. \(2019\)](#).

Table 1 presents the orbital parameters of asteroids under investigation from the Small Body Database¹.

Table 2 contains their physical parameters from the same source.

Table 1. Elements of the orbits. The columns sequentially list: The object number, the size of the semi-major axis of the orbit a , its eccentricity e , its inclination to the line of sight i , the longitude of the ascending node W , the argument of perihelion w , the Earth Minimum Orbit Intersection Distance (MOID), the Jupiter MOID, and the Jupiter Tisserand invariant T_j .

| Object | a | e | i | W | w | Earth MOID | Jupiter MOID | T_j |
|--------|-------|-------|--------|---------|---------|---------------|-----------------|-------|
| | au | | deg | deg | deg | au | au | |
| 8355 | 2.336 | 0.288 | 7.705 | 154.140 | 196.326 | 0.657 | 2.425 | 3.499 |
| 9773 | 2.681 | 0.388 | 14.700 | 277.512 | 15.582 | 0.628 | 1.507 | 3.221 |
| 32575 | 2.225 | 0.337 | 2.232 | 229.088 | 98.305 | 0.465 | 2.395 | 3.569 |
| 97679 | 1.571 | 0.132 | 50.815 | 196.325 | 138.410 | 0.403 | 3.539 | 4.001 |
| 122463 | 2.162 | 0.321 | 8.716 | 157.614 | 158.169 | 0.458 | 2.478 | 3.613 |
| 313591 | 2.382 | 0.423 | 11.885 | 312.090 | 32.101 | 0.382 | 2.086 | 3.384 |

Information about the observations is presented in Table 3.

The details of our observations' method and analysis technique are described in [Volkov et al. \(2019\)](#) and [Barabanov et al. \(2019\)](#). The transformation coefficients from the instrumental system to the standard one were published in [Barabanov et al. \(2021b\)](#). Some previous results on asteroids 8355, 9773, and 32575 were published in [Barabanov et al. \(2021a\)](#). For taxonomy derivation, a

¹https://ssd.jpl.nasa.gov/tools/sbdb_lookup.html

Table 2. Physical parameters. The columns sequentially list: The object number, the absolute stellar magnitude, its diameter D , the geometric albedo and the rotation period P .

| Object | Absolute mag | D , km | Albedo | P , hours |
|--------|--------------|----------|--------|-------------|
| 8355 | 14.40 | 3.874 | 0.277 | 6.0677 |
| 9773 | 13.79 | 4.016 | 0.377 | 2.74595 |
| 32575 | 15.42 | 2.157 | 0.325 | 4.5344 |
| 97679 | 16.64 | - | - | - |
| 122463 | 15.59 | - | - | 426 |
| 313591 | 16.56 | - | - | - |

Table 3. Observation log. The columns sequentially list: The object, the observation date, the heliocentric distance r , the geocentric distance Δ , the phase angle α , exposure times and the number of frames.

| Object | Date (JD) | r (au) | Δ (au) | α (deg) | exposure (sec) | Frames |
|--------|-----------|----------|---------------|----------------|----------------|--------|
| 8355 | 2456918 | 1.6691 | 0.6717 | 7.7 | 30-120 | 283 |
| 9773 | 2457242 | 1.6604 | 0.6828 | 15.0 | 30-60 | 160 |
| | 2457248 | 1.6687 | 0.7099 | 17.7 | 30-60 | 314 |
| | 2457249 | 1.6702 | 0.7149 | 18.1 | 30-60 | 402 |
| | 2457250 | 1.6718 | 0.7202 | 18.6 | 30-60 | 160 |
| 32575 | 2456881 | 1.4762 | 0.4642 | 6.3 | 60 | 160 |
| | 2456882 | 1.4757 | 0.4634 | 5.9 | 60-150 | 224 |
| 97679 | 2456937 | 1.3951 | 0.4074 | 12.7 | 20-60 | 649 |
| | 2456939 | 1.3972 | 0.4076 | 11.5 | 30-60 | 745 |
| | 2456940 | 1.3983 | 0.4087 | 11.3 | 30-40 | 503 |
| | 2456942 | 1.4005 | 0.4127 | 11.8 | 20-60 | 593 |
| 122463 | 2457611 | 1.4686 | 0.4593 | 7.1 | 60-80 | 57 |
| | 2457612 | 1.4687 | 0.4597 | 7.2 | 60-80 | 112 |
| | 2457613 | 1.4690 | 0.4603 | 7.3 | 60-80 | 83 |
| 313591 | 2456884 | 1.3830 | 0.4289 | 26.1 | 120-180 | 96 |
| | 2456885 | 1.3819 | 0.4263 | 25.8 | 120-180 | 104 |
| | 2456886 | 1.3810 | 0.4238 | 25.5 | 120-180 | 136 |

set of standard spectra of taxonomic classes were used, see [Tholen \(1989\)](#) and [Tholen \(1984\)](#).

3. Processing of observations.

Our multicolor observations made it possible to determine with sufficient accuracy the apparent stellar magnitudes and color indices of asteroids - see Table 4. The choice of reference stars in each frame satisfies the following conditions: the stars should be sufficiently bright (10^m-12^m), their color indices $B - V < 1.2$ and they should be located at the same frame with the asteroid (Barabanov et al. (2021b)). The number of reference stars in a single frame satisfying these conditions varied from 1 to 4. We interpolated tables from Straizys (1992) to find $V - Rc$, $Rc - Ic$ color indices of each reference star according to its $B - V$ color index derived from B , V magnitudes taken from the APASS DR10 catalogue².

Magnitudes of asteroid 8355, for technical reasons, were derived with only one reference star. In the case of asteroid 32575, the error obtained from observations seems to be underestimated.

Table 4. Stellar magnitudes of asteroids in $BVRcIc$ and their color indices with errors.

| Object | B | V | Rc | Ic | $B-V$ | $V-Rc$ | $V-Ic$ |
|--------|-------|-------|-------|-------|-------|--------|--------|
| 8355 | 16.29 | 15.36 | 14.80 | 14.41 | 0.93 | 0.56 | 0.95 |
| | 0.08 | 0.15 | 0.22 | 0.23 | 0.09 | 0.08 | 0.1 |
| 9773 | 16.01 | 15.10 | 14.61 | 14.25 | 0.91 | 0.48 | 0.85 |
| | 0.08 | 0.15 | 0.22 | 0.23 | 0.09 | 0.08 | 0.1 |
| 32575 | 16.06 | 15.23 | 14.82 | 14.46 | 0.84 | 0.41 | 0.77 |
| | 0.03 | 0.02 | 0.02 | 0.04 | 0.05 | 0.02 | 0.06 |
| 97679 | 17.22 | 16.29 | 15.83 | 15.50 | 0.93 | 0.46 | 0.79 |
| | 0.13 | 0.12 | 0.07 | 0.09 | 0.06 | 0.07 | 0.07 |
| 122463 | 16.11 | 15.21 | 14.93 | 14.33 | 0.91 | 0.27 | 0.88 |
| | 0.06 | 0.02 | 0.08 | 0.08 | 0.07 | 0.08 | 0.16 |
| 313591 | 17.28 | 16.57 | 16.23 | 15.90 | 0.72 | 0.33 | 0.66 |
| | 0.05 | 0.05 | 0.1 | 0.13 | 0.04 | 0.08 | 0.1 |

A set of standard spectra of taxonomic classes we construct using Tholen (1984) description. We transferred stellar magnitudes in different spectral ranges to energetic units, normalized them to the flow in the V band and compare with standard Tholen's spectra. The specific class of asteroids was determined by the minimum of the mean-square deviation of the coarse spectrum of the asteroid obtained from observations (four points) from the standard spectrum, as shown in the Figures with even numbers below.

Next, we present for each asteroid the relative spectrum energy distribution and phased with rotational period light curves Table 5.

²<https://www.aavso.org/apass>

3.1. (8355) Masuo 1989 RQ1

(8355) Masuo 1989 RQ1 was discovered on September 5, 1989 at the Palomar Observatory by the American astronomer Eleanor Helin and named after Japanese astronomer Masuo Tanaka (University of Tokyo).

Our observations of this asteroid were carried out only for 5 hours, which makes it impossible to correct its period 6.0677 h – from Small Body Database³. We can only say that our observations do not contradict previous data, see Fig. 1. Estimates of the variability semi-amplitude in different spectral regions are: $A_B = 0.^m09$, $A_V = 0.^m1$, $A_{Rc} = 0.^m1$, $A_{Ic} = 0.^m09$. The distribution of energy in the spectrum best corresponds to the taxonomic class A - see Fig. 2. There is a relatively large mismatch in B due to its big error.

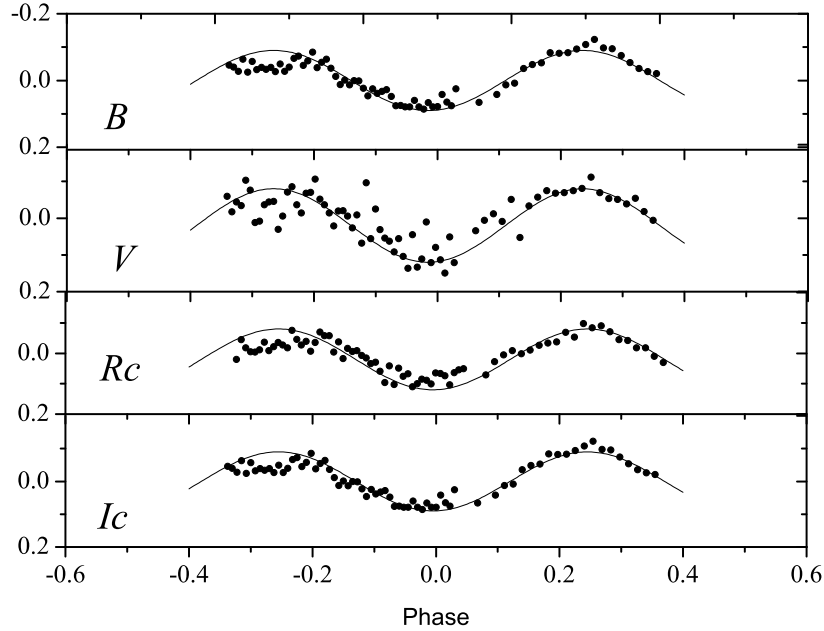


Figure 1. The phased light curve of 8355 asteroid in $BVRcIc$ bands. $P = 6.0677$ h. $B_{mean} = 16^m.29$, $V_{mean} = 15^m.36$, $Rc_{mean} = 14^m.80$, $Ic_{mean} = 14^m.41$. The solid curve corresponds to a sinusoid with a variability amplitude.

³https://ssd.jpl.nasa.gov/tools/sbdb_lookup.html

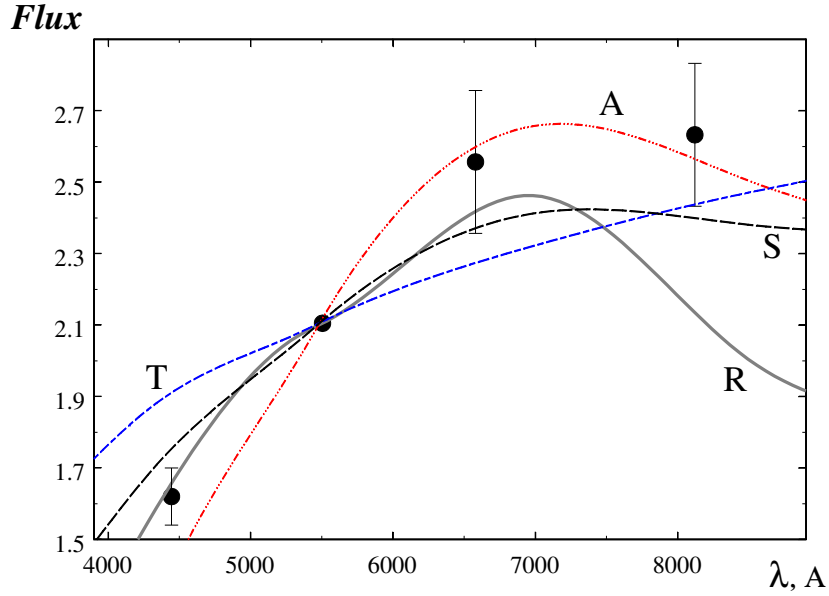


Figure 2. Energy distribution in the spectrum of asteroid 8355 Masuo. Dimensionless quantities are plotted along the y axis - the flux normalized to the solar one with a coefficient according to the works of Tholen. The curves of different colors correspond to some of the indicated standard taxonomic classes according to Tholen (1989), Tholen (1984). Black circles with error bars are observed data. Everything is normalized to the flux in the V filter, so that this point is considered accurate (indicated without an error bar), and the inaccuracy of observations in V is taken into account in the flux errors in other spectral bands.

3.2. (9773) 1993 MG1

(9773) 1993 MG1 was discovered on June 23, 1993 at the Palomar Observatory by astronomer Eleanor Helin (E.F. Helin).

We have determined the value of the rotation period $P = 2.7461 \pm 0.0002$ hours - see Fig. 3, which confirms the value determined by Benishek & Brincat (2016) within their errors. We can't get better accuracy due to the short duration of our observations. Estimates of the variability semi-amplitude in different spectral regions are: $A_B = 0.^m11$, $A_V = 0.^m13$, $A_{Rc} = 0.^m13$, $A_{Ic} = 0.^m14$. The taxonomic class corresponds to the class S - see Fig. 4.

3.3. (32575) 2001 QY78

(32575) 2001 QY78 was discovered on August 16, 2001 as part of the LINEAR (Lincoln Near-Earth Asteroid Research) program at the Socorro Observatory,

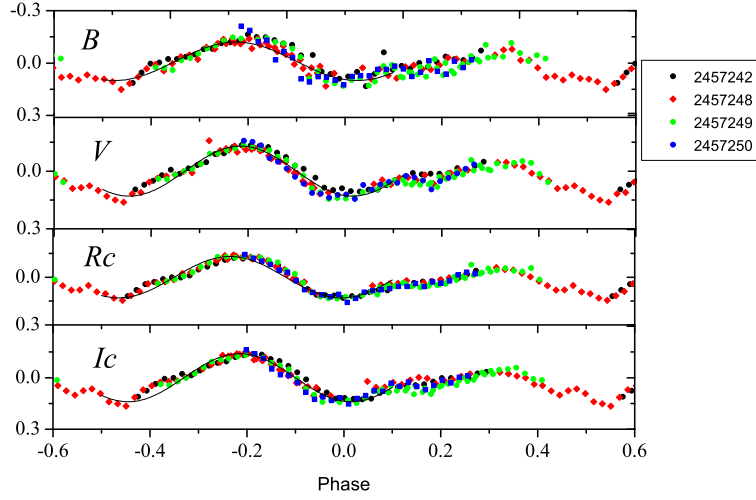


Figure 3. The phased light curve of 9773 asteroid in *BVRcIc* bands. $P = 2.74608$ h. $B_{mean} = 16^m.01$, $V_{mean} = 15^m.10$, $Rc_{mean} = 14^m.61$, $Ic_{mean} = 14^m.25$. Points of the same color correspond to one observation night: The legend shows correspondence between color and observation JD. The solid curve corresponds to a sinusoid with a variability amplitude.

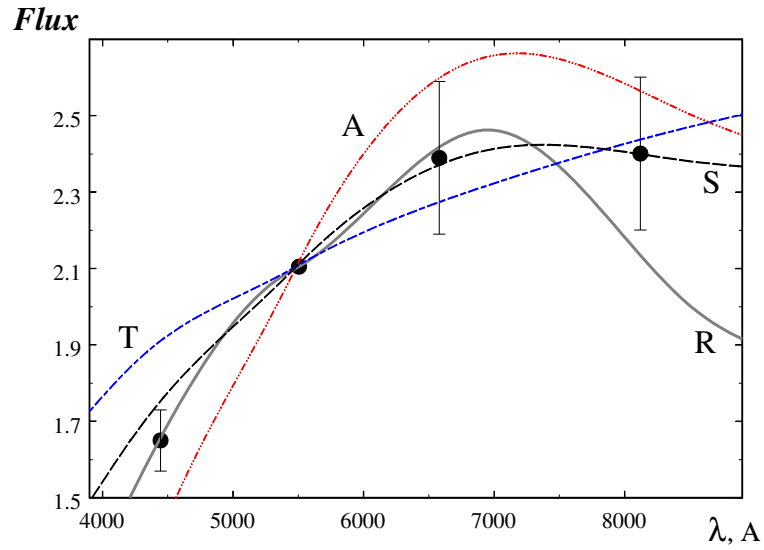


Figure 4. Energy distribution in the spectrum of asteroid 9773. Symbols are the same as in Fig. 2.

New Mexico.

The rotation period of the asteroid was determined by us as $P = 4.5331 \pm 0.0017$ hours, which coincides with previous measurements (4.5344 h – see the Small Body Database⁴) within errors. As in the case of asteroid 9733, increasing the duration of observations will improve the accuracy of the value of the rotation period. The phased light curve corresponding to the found period is shown in Fig. 5. Estimates of the variability semi-amplitude in different spectral regions are: $A_B = 0.^m41$, $A_V = 0.^m4$, $A_{Rc} = 0.^m4$, $A_{Ic} = 0.^m38$. From *BVRcIc* photometry, the value of the taxonomic class Q is obtained, see Fig. 6.

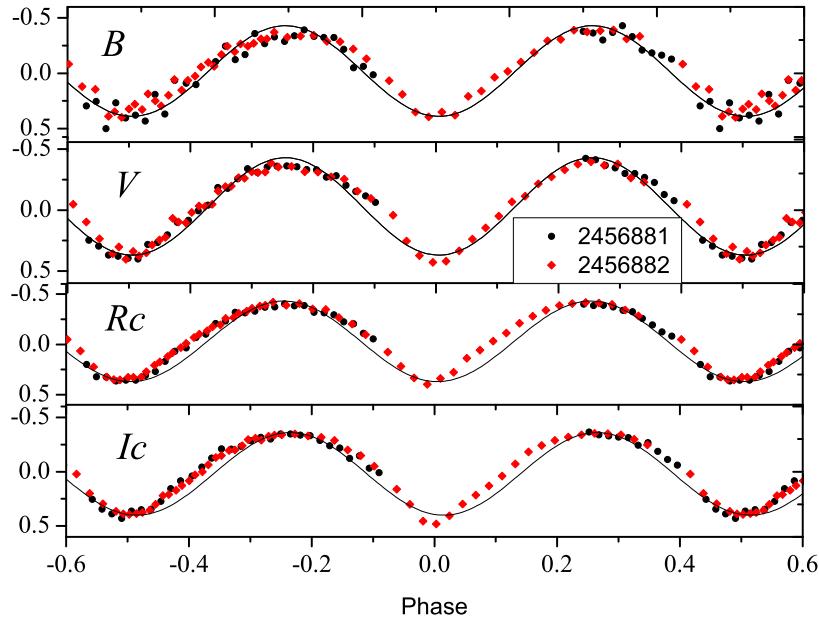


Figure 5. The phased light curve of 32575 asteroid in *BVRcIc* bands. $P = 4.53312$ h. $B_{mean} = 16^m.06$, $V_{mean} = 15^m.23$, $Rc_{mean} = 14^m.82$, $Ic_{mean} = 14^m.46$. Points of the same color correspond to one observation night: The legend shows correspondence between color and observation JD. The solid curve corresponds to a sinusoid with a variability amplitude.

3.4. (313591) 2003 MB7

(313591) 2003 MB7 was discovered on June 28, 2003 as part of the LINEAR program at the Socorro Observatory, New Mexico.

⁴https://ssd.jpl.nasa.gov/tools/sbdb_lookup.html

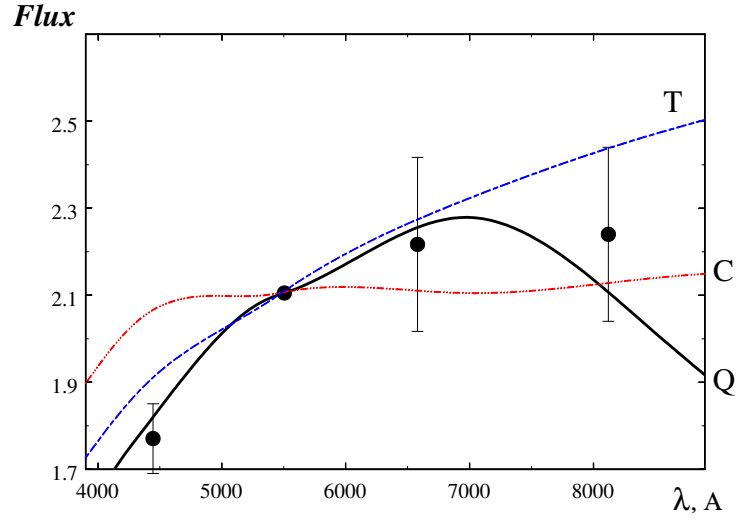


Figure 6. Energy distribution in the spectrum of asteroid 32575. Symbols are the same as in Fig. 2.

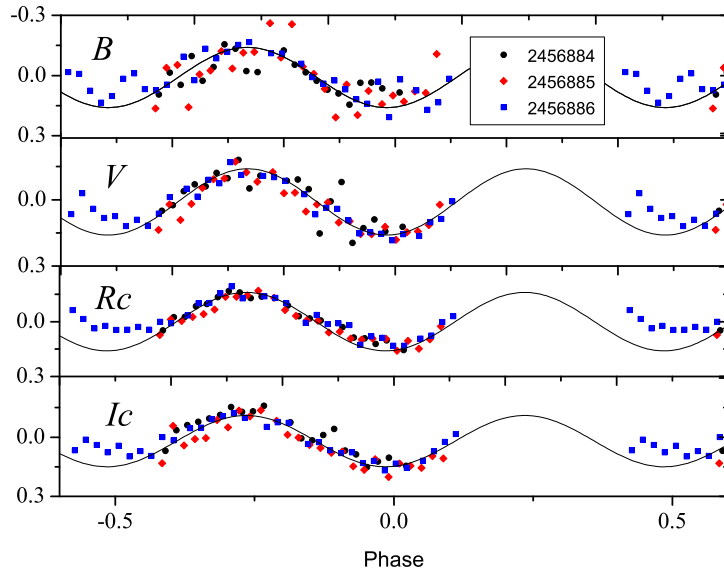


Figure 7. The phased light curve of 313591 asteroid in *BVRcIc* bands. $P = 7.92$ h. $B_{mean} = 17^m.28$, $V_{mean} = 16^m.57$, $Rc_{mean} = 16^m.23$, $Ic_{mean} = 15^m.90$. Points of the same color correspond to one observation night: The legend shows correspondence between color and observation JD. The solid curve corresponds to a sinusoid with a variability amplitude.

We estimated the value of the period $P \approx 7.92$ hours, see Fig. 7. The periodogram built with our program (Volkov, 2022) shows two approximately equal peaks at the given period value and at 6.85 hours. After close examination of phased with these periods light curves, we have chosen the larger one as it has less systematic deviations. It is impossible to determine the precise value of the period from the available data. The final conclusion can be made only after additional observations. Estimates of the variability semi-amplitude in different spectral regions are: $A_B = 0.^m15$, $A_V = 0.^m15$, $A_{Rc} = 0.^m16$, $A_{Ic} = 0.^m14$. Very accurate values of the color indices of the asteroid have been obtained, they correspond to Tholen's taxonomic class C, see Fig. 8.

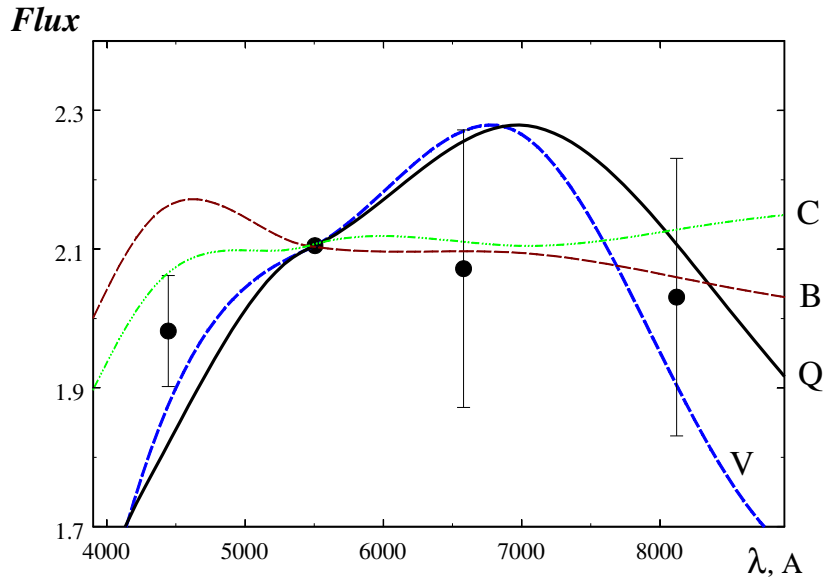


Figure 8. Energy distribution in the spectrum of asteroid 313591. Symbols are the same as in Fig. 2.

3.5. (97679) 2000 GG2

(97679) 2000 GG2 was discovered on April 3, 2000 as part of the LINEAR program at the Socorro Observatory, New Mexico. At the time of processing the observations, no physical and chemical parameters were known, except for the absolute magnitude, see Table 2. We have succeeded in detecting periodic variations in brightness, but the accuracy of observations is comparable to the amplitude of the variations, which can lead to an erroneous value of the rotation period, see Fig. 9. We consider this period to be 7.964 ± 0.004 hours. Further

observations will help to confirm this value. Estimates of the variability semi-amplitude in different spectral regions are: $A_B = 0.^m15$, $A_V = 0.^m15$, $A_{Rc} = 0.^m08$, $A_{Ic} = 0.^m12$.

Multicolor observations have allowed us to determine the taxonomic class of this asteroid as S, although there is a non-zero probability that it can also belong to the R class – see Fig. 10.

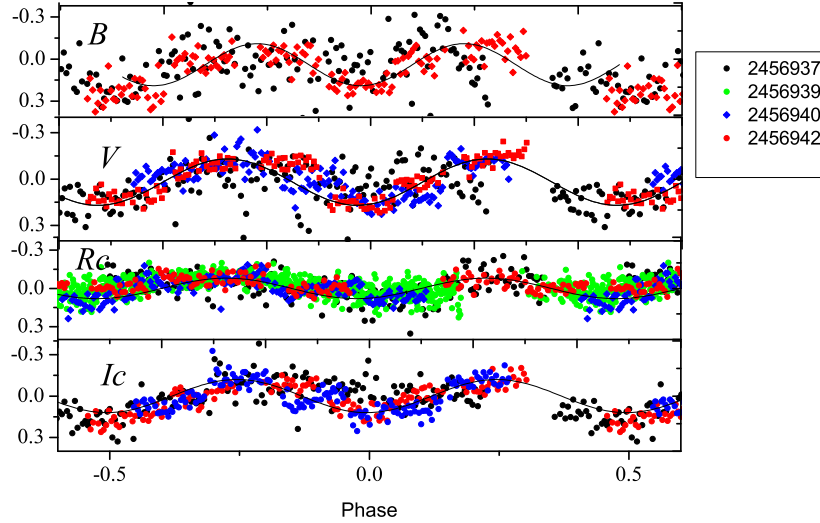


Figure 9. The phased light curve of 97679 asteroid in $BVRcIc$ bands. $P = 7.9644$ h. $B_{mean} = 17^m.22$, $V_{mean} = 16^m.29$, $Rc_{mean} = 15^m.83$, $Ic_{mean} = 15^m.50$. Points of the same color correspond to one observation night: The legend shows correspondence between color and observation JD. The solid curve corresponds to a sinusoid with a variability amplitude.

3.6. (122463) 2000 QP148

(122463) 2000 QP148 was discovered as part of the LINEAR program at the Socorro Observatory, New Mexico. The estimated value of the rotation period is 426.3 hours, i.e. more than 17 days, see Table 2, and examples of asteroid light curves⁵. With only three consecutive nights of observations at hand, we can neither confirm nor deny this value. Our observations are presented in Fig. 11. We did not find any brightness' fluctuations at times from tens of minutes to several hours. To accurately determine the rotation period, it is necessary to organize systematic observations of this object during several months. The distribution of energy in the spectrum is shown in Fig. 12. We believe that the Tholen taxonomic class of this asteroid corresponds to the T class.

⁵<https://www.asu.cas.cz/asteroid/122463.png>

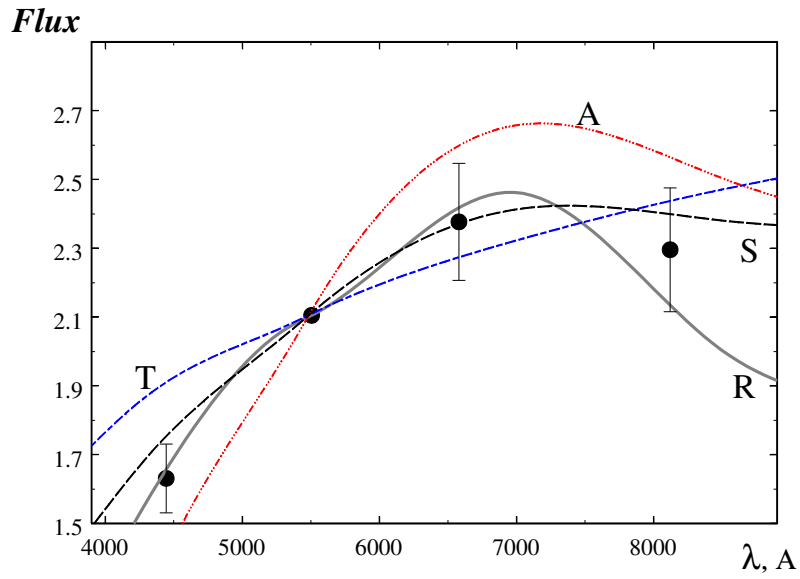


Figure 10. Energy distribution in the spectrum of asteroid 97679. Symbols are the same as in Fig. 2.

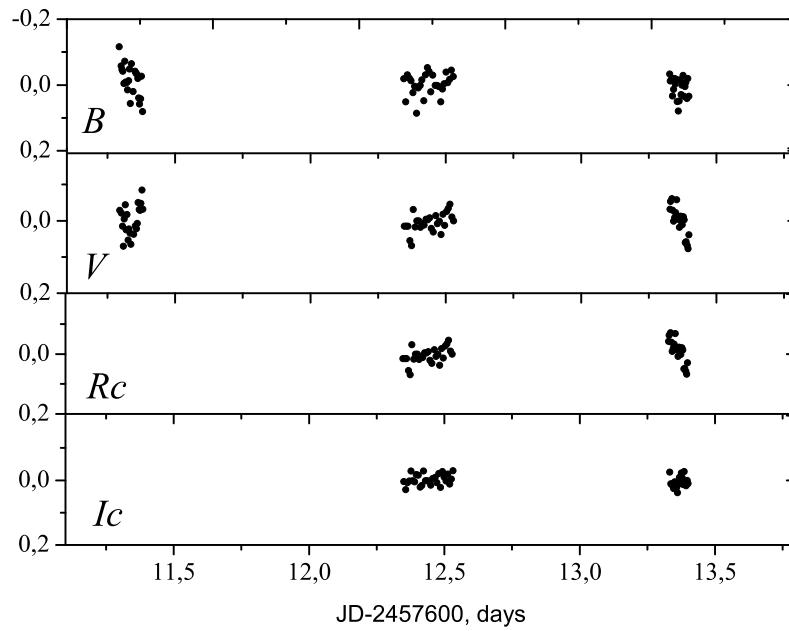


Figure 11. The non-phased light curve of 122463 asteroid in $BVRcIc$ bands. $B_{mean} = 16^m.11$, $V_{mean} = 15^m.21$, $Rc_{mean} = 14^m.93$, $Ic_{mean} = 14^m.33$.

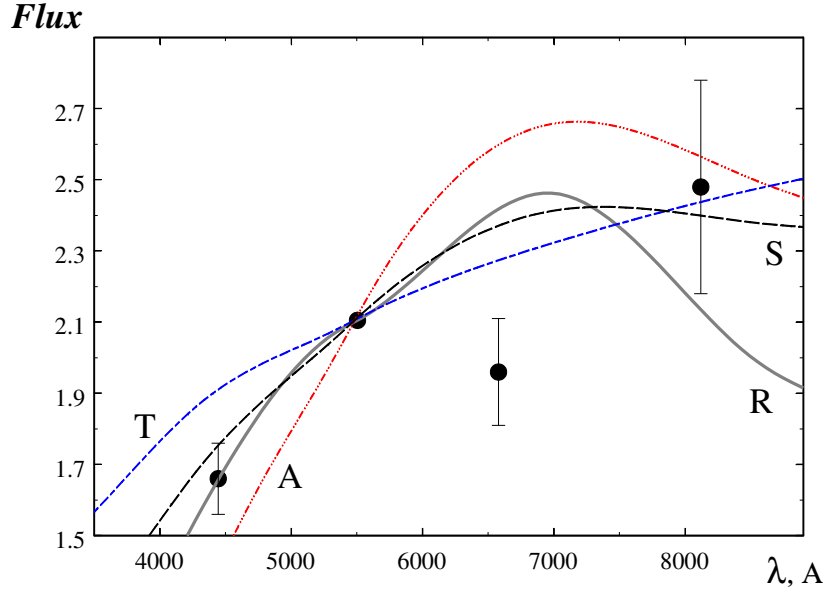


Figure 12. Energy distribution in the spectrum of asteroid 122463. Symbols are the same as in Fig. 2.

Table 5. The rotation period P , the magnitude in the V band (with error), and the Tholen taxonomy.

| Object | P , hours | V (err), mag | Taxonomy according Tholen |
|--------|--------------|----------------|---------------------------|
| 8355 | - | 15.36 (15) | A |
| 9773 | 2.74608 (24) | 15.10 (15) | S |
| 32575 | 4.53312 (17) | 15.23 (2) | Q |
| 97679 | 7.9644 (36) | 16.29 (12) | S |
| 122463 | - | 15.21 (2) | T |
| 313591 | 7.92 (2) | 16.57 (5) | C |

4. Conclusion

Photometric multicolor high-precision observations of six Mars-crossing asteroids were made with the Zeiss-1000 telescope in Simeiz during 2014–2016. For all of them, apparent stellar magnitudes and color indices were obtained, and an assessment of the taxonomic class according to Tholen was made. For asteroids 97679 and 313591 the period of proper rotation was estimated for the first time. For asteroids 9773 and 32575 our independent determination of the rotation pe-

riod coincides with the previous estimates within their errors. Asteroid 122463 requires a long (several months) monitoring to determine the value of the rotation period. Undoubtedly, targeted photometric observations of Mars-crossing asteroids will make it possible to determine their origin. These observations will have not only scientific but also obvious practical value.

Acknowledgements. This work has been supported by SAIA scholarship (ASK, IMV).

References

- Barabanov, S. I., Kravtsova, A. S., Volkov, I. M., & Bakanas, E. S., Observations of Mars-crossing asteroids with 1-m telescope of Simeiz Observatory of INASAN. 2021a, *INASAN Science Reports*, **6**, 88, DOI: 10.51194/INASAN.2021.6.3.005
- Barabanov, S. I., Potanin, S. A., Savvin, A. D., et al., Focus reducer for the Zeiss-1000 telescope of the Simeiz group Zvenigorod Observatory INASAN. 2021b, *INASAN Science Reports*, **6**, 92, DOI: 10.51194/INASAN.2021.6.3.006
- Barabanov, S. I., Volkov, I. M., Kravtsova, A. S., Nikolenko, I. V., & Kryuchkov, S. V., Photometric investigations of NEA in Institute of Astronomy of the RAS in 2008-2010. 2019, *INASAN Science Reports*, **4**, 278, DOI: 10.26087/INASAN.2019.4.2.042
- Benishek, V. & Brincat, S. M., Rotation Period Determination for (9773) 1993 MG1. 2016, *Minor Planet Bulletin*, **43**, 90
- Nikolenko, I. V., Kryuchkov, S. V., Barabanov, S. I., & Volkov, I. M., Telescopes of the INASAN Simeiz Observatory: current state and prospects. 2019, *INASAN Science Reports*, **4**, 85, DOI: 10.26087/INASAN.2019.4.2.015
- Straizys, V. 1992, *Multicolor stellar photometry*
- Tholen, D. J. 1984, Asteroid Taxonomy from Cluster Analysis of Photometry., PhD thesis, University of Arizona
- Tholen, D. J., Asteroid taxonomic classifications. 1989, in *Asteroids II*, ed. R. P. Binzel, T. Gehrels, & M. S. Matthews, 1139–1150
- Volkov, I. M., V961 Cep - a new eclipsing variable with δ Sct component. 2022, *Pere-mennyye Zvezdy*, **42**, 1, DOI: 10.24412/2221-0474-2022-42-1-7
- Volkov, I. M., Barabanov, S. I., Nikolenko, I. V., Kryuchkov, S. V., & Sergeev, A. V., Spectral observations and photometry of the near-Earth object (25916) 2001 CP44. 2019, *Contributions of the Astronomical Observatory Skalnaté Pleso*, **49**, 301